

RESEARCH PAPER

D.P. Adhikari · F. Kumon

Climatic changes during the past 1300 years as deduced from the sediments of Lake Nakatsuna, central Japan

Received: February 16, 2001 / Accepted: June 7, 2001

Abstract Limnological features and sediment characteristics were studied in Lake Nakatsuna, a mesotrophic lake in central Japan. The lake is dimictic, and is anoxic in the hypolimnion during thermal stratification from May to September. In an attempt to reconstruct paleoclimatic changes around the lake, a sediment core taken from the lake center spanning the past 1300 years was analyzed for its organic and inorganic contents. Climatic influences were examined on the variation of total organic carbon (TOC), total nitrogen (TN), and sand contents. Short- and long-term fluctuations in TOC, TN, and sand contents are evident, and variation in atmospheric temperature appears to be important for their long-term variability. The sediment record from AD 900 to 1200 indicates hot summers and warm winters with less snow accumulation, whereas the record from AD 1200 to 1950 is characterized by high variation of temperature, with three cool phases from AD 1300 to 1470, 1700 to 1760, and 1850 to 1950. The warm period from AD 900 to 1200 corresponds well to the Medieval Warm Period, and the second and third cool phases are related to the Little Ice Age.

Key words Nishina Three Lakes · Organic carbon · Climatic proxy · Medieval Warm Period · Little Ice Age

Introduction

Climate change is a growing concern whether naturally or anthropogenically induced. In this regard, an important goal of paleoclimatic research is to understand the natural

variability in the climate system over time. Instrumental climate records alone cannot be used toward this objective, because they do not go back far enough in time. Thus, paleoclimate researchers must rely on proxy climate indicators combined with available instrumental or historical records to obtain information on long-term climate changes. Among the key environments that provide potential multi-proxy sources, lake sediments are becoming an increasingly common and important sensor to record climate signals.

Researches carried out in the past years in and around central Japan provide results of paleoclimatic reconstruction from the sediments of a number of larger lakes (e.g. Fukusawa 1995; Inouchi et al. 1996; Kumon et al. 2000; Kumon 2001). However, Lake Nakatsuna has received no mention in the past, most probably due to its smaller size. Despite its size, the understanding of its response to climate change is of interest, because every lake responds in a specific manner, as controlled by its own hydraulic conditions and the surrounding environment. Lake Nakatsuna is an intermontane lake with short wind fetch. The rivers flowing into the lake are few and small, and there are no strong waves or currents redistributing the sediments in its center. Thus, the depositional environment in the lake is relatively calm, and the sediment is expected to be homogeneous, with little flood input. The sediments from Lake Nakatsuna are therefore suitable for paleoclimatic studies.

The prime objectives of this study were to reveal the modern limnological characteristics of the lake as a basis for interpretation of sediment characteristics and to investigate the response of sediment to paleoclimatic change over time. The approach adopted here rests upon the measurement of total organic carbon (TOC), total nitrogen (TN), and sand content, which gives a qualitative assessment of paleoclimate. Climatic reconstructions obtained by resolving these proxies are then compared with the historical climate records. This study contributes to a better understanding of the Medieval Warm Period (MWP) and of the Little Ice Age (LIA) and adds to our understanding of high-resolution paleoclimatic changes in central Japan over the past 1300 years.

D.P. Adhikari (✉)¹ · F. Kumon
Department of Environmental Sciences, Faculty of Science, Shinshu University, Asahi 3-1-1, Matsumoto 390-8621, Japan
Tel. +81-0263-37-2479; Fax +81-0263-37-2560
e-mail: adhikaridp@hotmail.com

Permanent address:

¹Tribhuvan University, Tri-Chandra Campus. Department of Geology, P.O. Box 13644, Kathmandu Nepal

Study area

Lake Nakatsuna is located in a narrow intermontane valley extending N-S from Hakuba to Omachi City near the northern Japanese Alps in Nagano Prefecture, central Japan. The lake is the smallest (0.125 km²) and central lake of a series of three freshwater bodies known as the Nishina Three Lakes (Fig. 1). The drainage basin of this lake covers 3.70 km² of forest, grassland including a skiing area, and rice fields, and the elevation ranges from 820 to 1330 m (Table 1).

Within the watershed, the western mountains consist mainly of granite and welded tuffs of Cretaceous age, whereas the eastern mountains consist of Tertiary sedimentary rocks and late Quaternary terrace deposits. The geology of the drainage basin is well reflected in its morphology, as high relief and steep slopes prevail to the west and low-lying gentle topography predominates to the east (Fig. 1). The Itoigawa-Shizuoka Tectonic Line, a well-known boundary

fault, runs through this valley, and the formation of these lakes has a genetic relation with this active fault system.

The nearest meteorological station is located in Omachi City, ca. 10 km south of the lake. The Automated Meteorological Data Acquisition System (AMeDAS) records at Omachi site (Japanese Meteorological Agency) indicate that the annual average temperature over the past 28 years varied from 8.3° to 10.5°C. The average summer temperature (June to September) shows a narrow variation from 18° to 21°C, compared with the winter average (December to March), which ranges from 1.1° to -5.2°C (Fig. 2). The annual average precipitation for the same period is 1334 mm, with a large variation from year to year. Although the winter precipitation is relatively constant (290 mm), the summer precipitation varies more. A negative correlation exists between total annual precipitation and annual average temperature (Fig. 2), and it is particularly apparent between summer precipitation and summer average temperature (Fig. 3).

Fig. 1. Location of Lake Nakatsuna and its watershed. Lake Kizaki and Omachi City are to the south of this map. Dashed lines show watershed boundary. Topographic contour interval is 100 m. Adapted from the topographic map, 1:25 000, Kamishiro (Geographical Survey Institute of Japan)

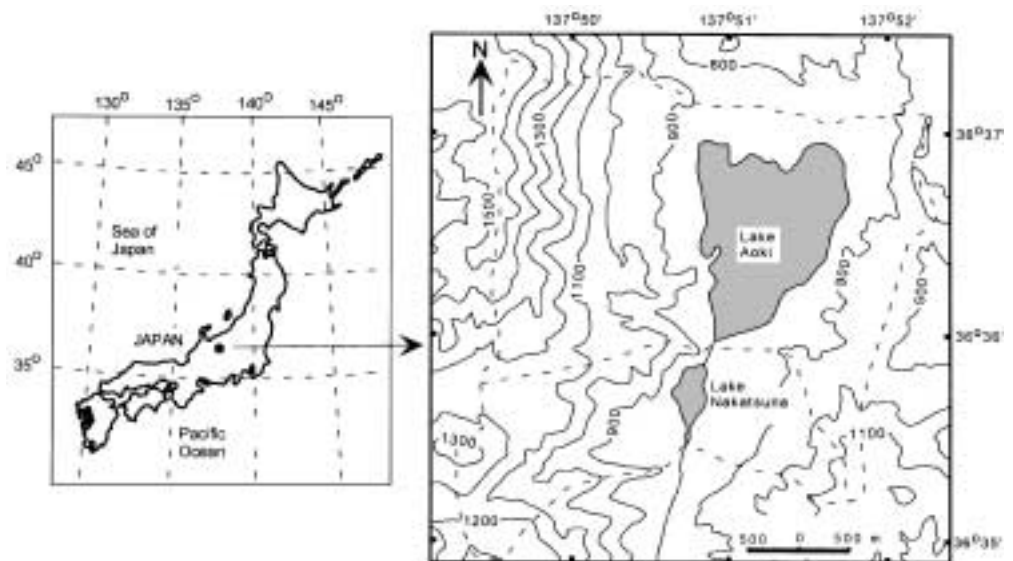


Table 1. Physical characteristics of Lake Nakatsuna and its drainage basin (Horie 1962)

Altitude	820 m
Surface area	0.125 km ²
Area of drainage basin	3.7 km ²
Maximum relief in drainage area	510 m
Perimeter	1.86 km
Length (max)	675 m
Breadth (max)	325 m
Depth (max)	~15 m
Mean depth	~8 m
Water volume	~798 × 10 ³ m ³
Water residence period	25 days

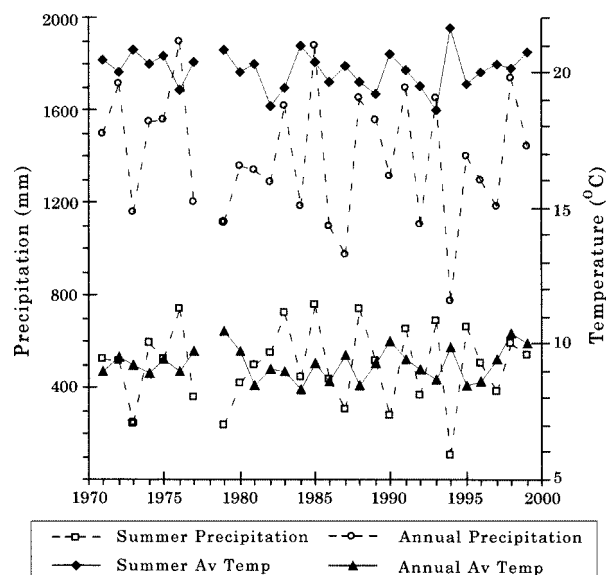


Fig. 2. Variation in temperature and precipitation during the last 28 years at Omachi City, Nagano Prefecture (after Japanese Meteorological Agency)

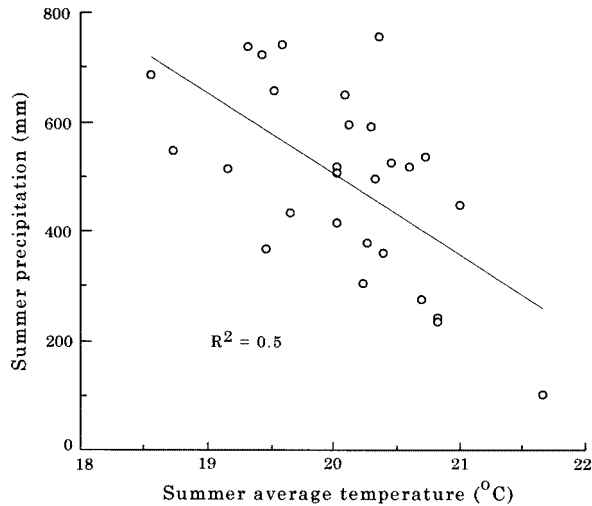


Fig. 3. Relationship between summer average temperature and summer precipitation during the last 28 years at Omachi City, Nagano Prefecture (after Japanese Meteorological Agency)

Limnology

The basin floor of Lake Nakatsuna trends N-S with steeper (5° – 10°) margins on the northern, eastern, and western sides, and a gentler (2° – 4°) margin on the southern side (Fig. 4). The maximum dimensions of the lake are $675 \times 325 \times 15$ m. The water volume is about 798×10^3 m³, and the residence period under normal flow conditions is about 25 days (Horie 1962).

Of the three major tributary rivers, the Upper Nogu River flows from Lake Aoki into Lake Nakatsuna at its northern end. After 1954, artificial flow introduced from another river system for hydropower generation has been added to this river in winter and spring. A second western tributary, which historically entered the southwestern part of the lake, now enters the lake near its southern extremity close to its outlet sill. Consequently, this tributary has had little influence on the lake sediments recently. The third major tributary from the east flows into the lake west of Kojihara and supplies a major portion of the lake sediments. Additional small, perennial and ephemeral streams also flow into the lake. The lake drains into Lake Kizaki through the Middle Nogu River.

Records of physical and chemical data, such as temperature, dissolved oxygen (DO), pH, and turbidity, are very limited for Lake Nakatsuna. Therefore, we have added some measurements from February to August 2000 using a Water Quality Checker (Horiba U-10). The thermocline in the water column is established in June and disappears in October (Fig. 5). During this period, surface water temperatures generally stand well above 4°C and warm water ranging from 10° to 25°C stratifies above cool water of 5° to 8°C . The thermocline exists at depths of 5 to 10 m. In winter the water temperatures remain around 4°C , except for the uppermost 1 m, which is at nearly 0°C . The lake surface freezes for several weeks each year. Therefore, Lake Nakatsuna is a dimictic lake in which the entire body of

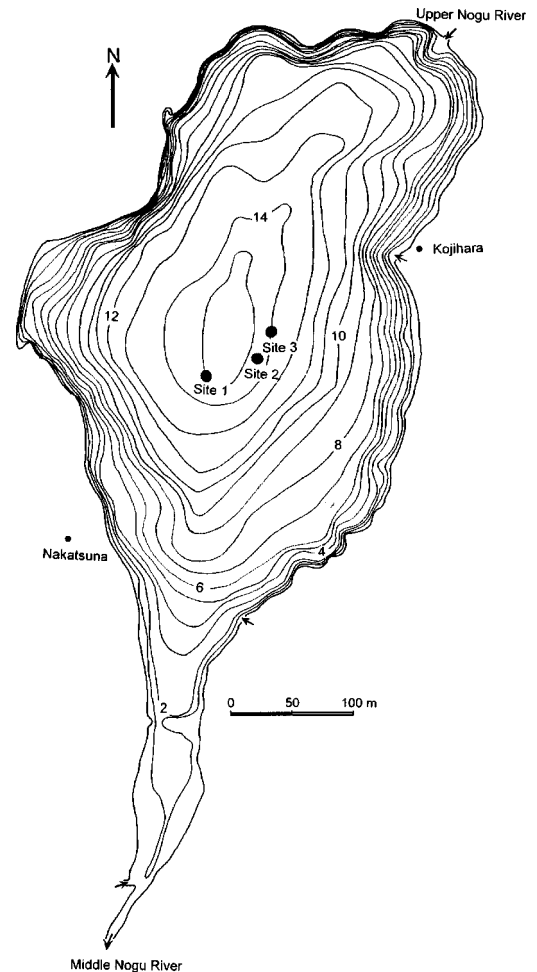


Fig. 4. Bathymetry of Lake Nakatsuna with the location of coring sites. Depth contours are in meters. This map was made by the students of the Japan Construction College in 1986, but the outline of the basin is somewhat deformed compared with the map by the Geographical Survey Institute of Japan

water circulates vertically twice a year, in late spring and late autumn.

DO in surface water ranges from 7 to 16 mg l⁻¹ from spring to autumn (Fig. 6). DO in the water column usually increases at mid-water depth, followed by a sharp decrease in the bottom horizon. The content varies from 16 mg l⁻¹ on the surface to 0 mg l⁻¹ at the bottom. The lowest DO content is invariably observed during summer (Fig. 6) because of the production of abundant organic matter, which consumes oxygen when it decomposes in the lower part of the stratified water column. The pH varies from 5 to 6.8, with an initial decrease followed by an increase in winter and vice versa in spring. Suspended sediment in the water column in winter and spring varies from 0.75 to 1.14 mg l⁻¹, with the highest content near the surface and the lowest at middle depths.

Bottom surface sediments

Samples of the top 5 cm of the bottom surface sediments were taken at 80 locations using a Birge-Ekman grab sam-

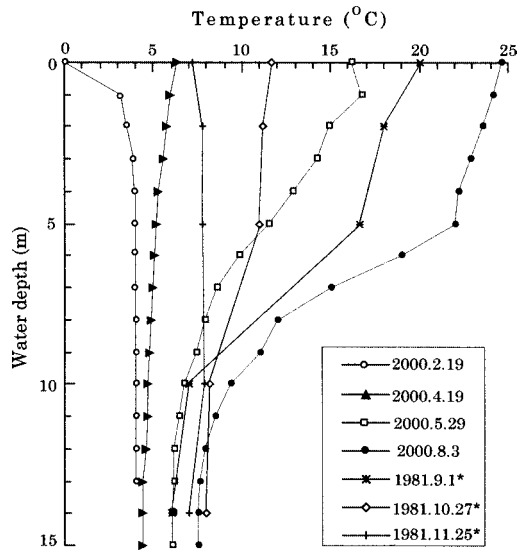


Fig. 5. Variation in temperature distribution in water column in Lake Nakatsuna. *Data from Nagano Research Institute for Health and Pollution (1983)

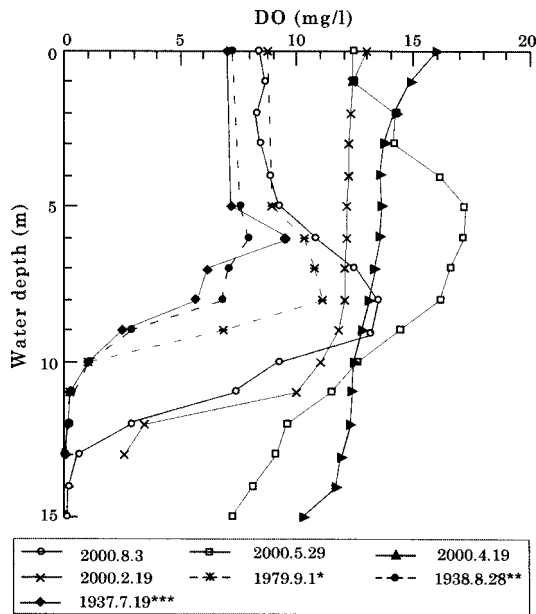


Fig. 6. Variation in dissolved oxygen (DO) with water depth in different months in Lake Nakatsuna. *Hayashi H. (personal communication); **Yoshimura (1938), and ***Sugawara et al. (1937)

pler (Fig. 7). Samples were examined for grain size, texture, and organic carbon and nitrogen contents. The grain size was analyzed by using the combined hydrometer and sieving method (Kumon et al. 1993). The nomenclature of sediment based on percentage composition of each sample for gravel, sand, silt, and clay is taken from Shepard (1954) (Fig. 8A).

There is a general correspondence between sediment grain size and water depth. Gravel and sand are restricted in the narrow shore zone, and the grain size decreases offshore, changing from sand through silty sand, sand silt clay to clayey silt or silty clay (Fig. 8B). Clayey silt and silty clay

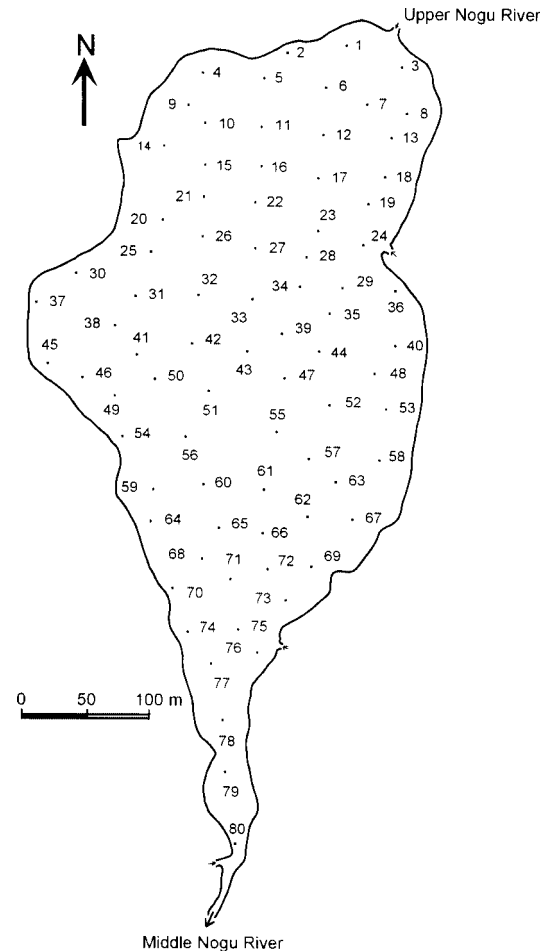


Fig. 7. Sampling location of surface sediments in Lake Nakatsuna

are the major components of the sediments on the basin floor, and silty clay is confined to the innermost part in three separate areas. Sortings of the sediments are poor to very poor and generally deteriorate with decreasing mean grain size. The distributions provide nonsymmetrical curves comprising one to three modal populations as gravel, sand, silt, and/or clay fractions (Fig. 9). Each mode is nearly symmetrical within itself, but variation of sorting within samples is high due to the addition of excess materials in the tail of the distribution curve.

HCl-treated specimens were measured for TOC and TN contents by using a CHN corder (Yanaco MT-5, Yanagimoto Seisakusho Co., Inc.). The TOC and TN contents vary from 0.6% to 7.3% and 0.05% to 0.55%, respectively, and have parallel distribution patterns (Fig. 10). The patterns are similar to the grain-size distribution, with increasing values from the inshore coarse-grained to the offshore fine-grained sediments (Fig. 8b). Both TOC and TN contents have strong negative and positive correlations with sand and clay contents, respectively. The C/N weight ratio ranges from 10 to 16, indicating mixing of lake plankton and terrestrial plant materials (Fig. 11). The C/N ratios are higher in the inshore zone and lower in the offshore sediments. This distribution is a key indicator for the evaluation of the detrital carbon input to the lake.

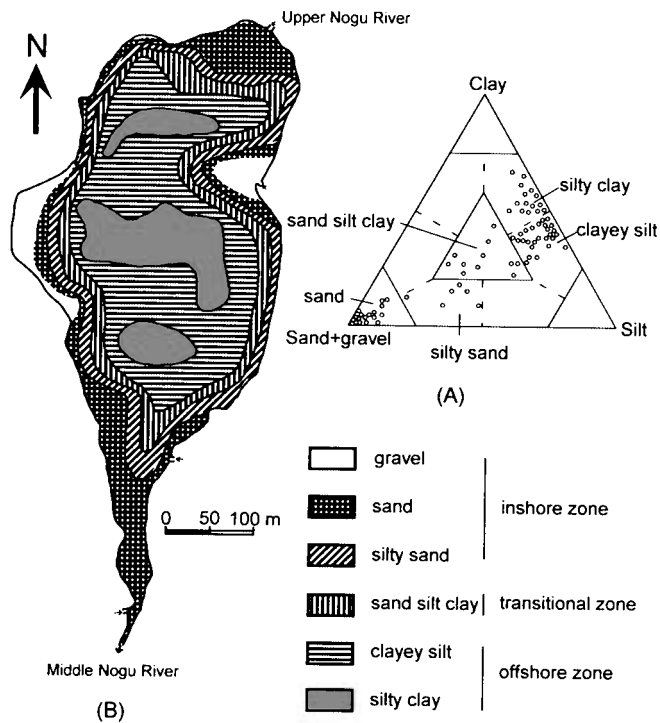


Fig. 8. Surficial sediments of Lake Nakatsuna. **A** Plots on the ternary diagram comprising sand plus gravel, silt, and clay as end members (Shepard 1954). **B** Distribution of sediments based on the nomenclature adopted in diagram A

Cored sediments

Three cores 315, 260, and 302 cm in length were taken from the central part of the lake at water depths of 15, 14.5, and 14 m, respectively, using a Mackereth piston core sampler (Natsuharagiken Co., Inc.) (Fig. 4). Sediment cores were recovered and split lengthwise in the laboratory. Lithology was described on the cut surface, and colors were assigned using Munsell soil color charts. The sediments were X-rayed to reveal internal sedimentary structures and sliced at 1-cm intervals for physical and chemical analyses. The uppermost 10 cm of the cored sediments was slightly disturbed by the coring and recovery processes. Recent climatic history was therefore examined by using a separate, 29-cm-long core extracted from the lake center with special care to keep the sediment–water interface intact.

Lithology

The sediments were almost dark-gray silty clay, with occasional intercalation of silt and/or sand layers in scales of millimeters to centimeters (Fig. 12). Based on X-ray photographs, granule and sand-size particles were sparsely scattered throughout the sediments, but varied among horizons (Fig. 13a). X-ray photographs also showed that some darker intervals (less transparent) had sharp basal boundaries and mud clasts were contained in the basal part (Fig. 13b). These mud clasts are less transparent balls or flakes smaller than 1 cm. Other intervals had contorted boundaries, which are interpreted as being slumped or slump-induced mass

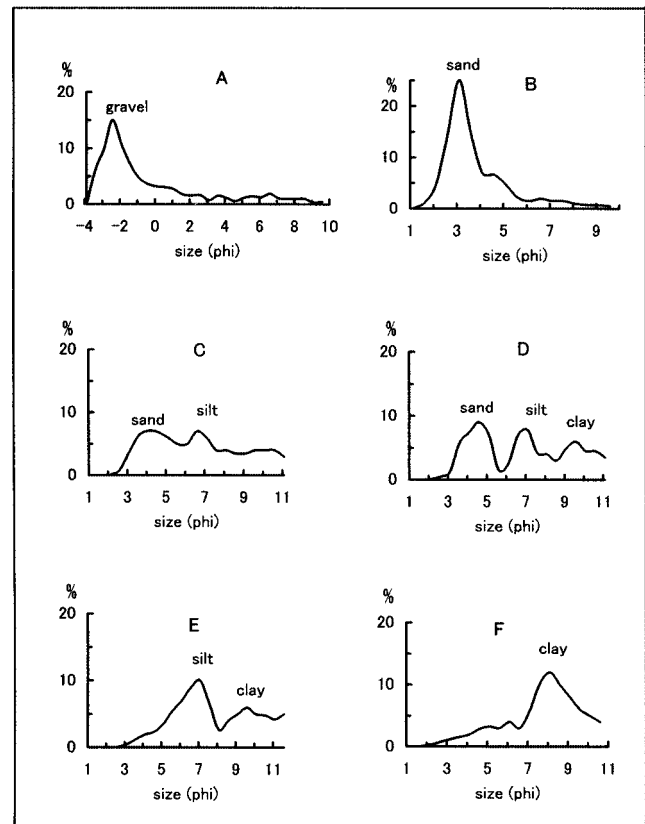


Fig. 9. Representative size-frequency curves to cover the inshore (**A**, **B**, **C**), transitional (**D**), and offshore (**E**, **F**) zones. Zones are indicated in Fig. 8B

flow structures (Fig. 13c). Fragments of terrestrial leaf and wood fragment were observed in some horizons. The core at site 1 was bottomed at a ca. 4-mm-thick clean sand layer. The three cores had similar lithology, with minor differences, and are correlative as shown in Fig. 12.

In the cored samples at sites 2 and 3, the boundaries of the strata were inclined, suggesting that the penetration of the core samplers was not vertical. Corrective factors are applied for these two cores to make them vertical, and the lengths mentioned above and shown in Fig. 12 are the corrected depths. The core at site 1 kept bedding planes horizontal and was the longest of the three cores. Therefore, we selected the cored sample at site 1 as representative of the three, and detailed analysis was performed on this sample only.

On the basis of smear slide observations at 2-cm intervals, sediments between 192 and 288 cm had the highest concentration of diatoms, dominated by *Tabellaria* and *Cyclotella*. Sediments above 192 and below 288 cm levels contained more diverse genera, such as *Aulacoseira*, *Cyclotella*, *Fragilaria*, *Navicula*, *Gomphonema*, *Amphora*, and *Surirella*, at low concentration. In addition, diatom concentrations were lower in the silty and sandy horizons than in the other clayey horizons.

Apparent density and sand content

Water content was measured as the difference in weight among freshly extruded samples before and after drying at

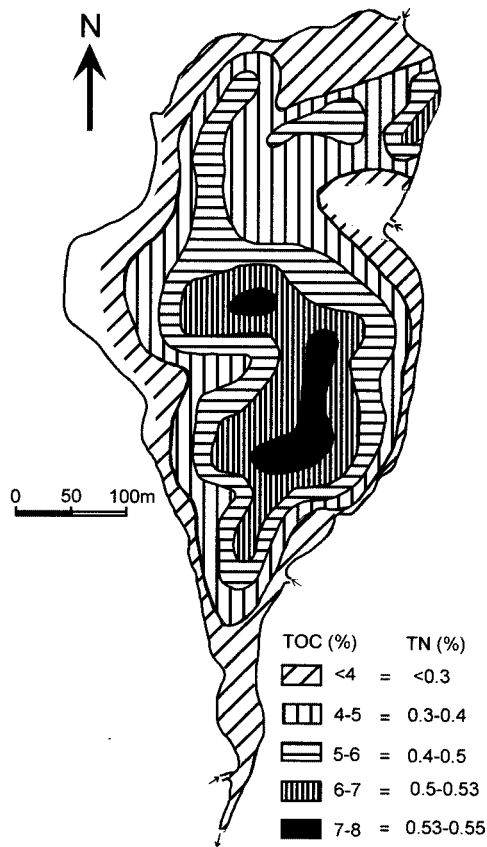


Fig. 10. Distribution of total organic carbon (TOC) and total nitrogen (TN) contents in the surface sediments of Lake Nakatsuna

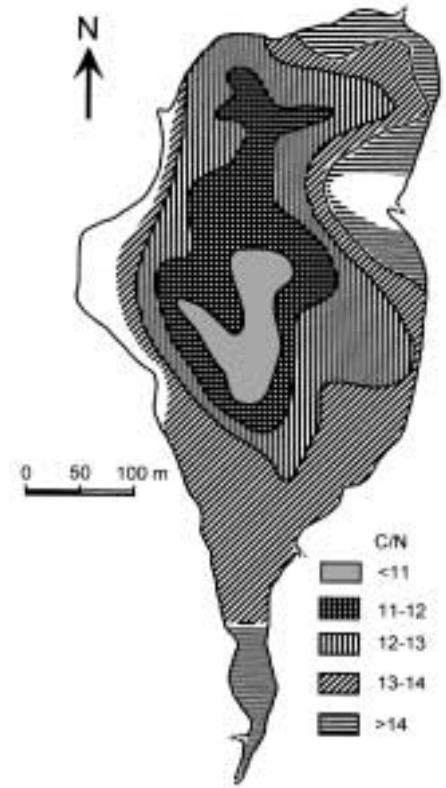


Fig. 11. Distribution of C/N ratios in the surface sediments of Lake Nakatsuna. C/N is the ratio of the total organic carbon to total nitrogen weight in each specimen

105°C for 12 h. The apparent density was calculated as solid weight per unit volume based on dry weight and water content, postulating grain density as 2.65 g cm^{-3} . The weighted dry samples were disaggregated by treating with hydrogen peroxide (H_2O_2) and were wet sieved on 4 and 4.5 phi sieves. Sediment fractions coarser than sand and coarse silt were quantified as the weight percent of 4 and 4.5 phi fractions to the original dry weight.

The water content and apparent density in the cored sediments varied from 50% to 80% and from 0.25 to 0.88 g cm^{-3} , respectively. The patterns of density variation were similar in the three cores, except in the lowermost part of the core at site 1, which had a much higher density (Fig. 14). Density slightly decreased downward in four steps. These steps are characterized by sudden increase at the base and gradual decrease upward. The basal parts of these steps usually have sharp basal boundaries, as identified by X-ray photographs.

Sand content usually varied from 0% to 2% and sometimes reached 15% (Fig. 15). Coarse silt content was very low and ranged from 0% to 0.8%. Within the given range, high sand content generally coincided with high coarse silt content, but an inverse relationship was rarely observed in some horizons. The short-term peaks in the density profile generally corresponded to the peaks in the sand and the coarse silt profiles. A single, small, pebble-size clast was encountered at 246 cm depth.

TOC, TN content, and C/N ratio

Dried samples were ground with an agate bowl and treated with diluted HCl (3%) to remove carbonate carbon. The samples were then dried two or three times, supplying distilled water at 110°C to remove the remaining HCl. Following the treatment, C, H, and N measurements were run using the dry combustion technique in a CHN coder (Yanaco MT-5), and the contents of TOC and TN were expressed in weight percentage of dry weight of original sediments.

TOC and TN showed variations from 8% to 15% and from 0.2% to 1%, respectively, whereas C/N ratios varied from 11 to 16 (Fig. 16). In these variations, TOC and TN profiles showed both short- and long-term fluctuations with parallel increases or decreases. Horizons containing exceptionally low TOC and TN correspond with event sediments at depths of 15, 78, 180, 270, and 300–315 cm. This low content is due to the dilution effect caused by sudden mixing of nonorganic or low-organic materials. Except for these horizons, the interval from 262 to 186 cm was characterized by abundant TOC and TN with high C/N ratios. The interval between 186 and 78 cm had significantly lower TOC and slightly higher TN contents. TOC content above 78 cm further decreased following the initial increase, whereas TN content varied less.

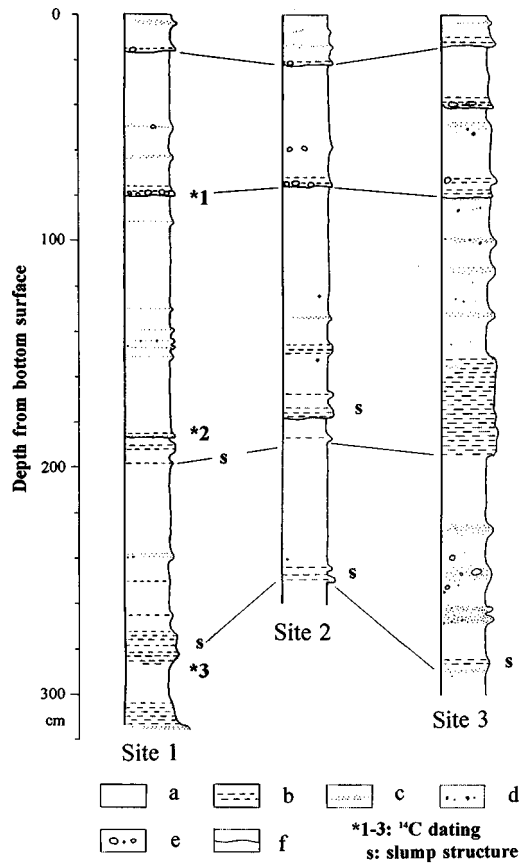


Fig. 12. Lithologic column of the three cores. **a** Silty clay layer, **b** silt layer, **c** sand grains, **d** scattered granule grains, **e** mud clasts, **f** sharp boundary; *1: 510 ± 40 YBP, *2: 670 ± 40 YBP, and *3: 1320 ± 40 YBP

Age of cored sediment

Radiocarbon dating was performed for one plant material and two organic sediments at the depths of 78, 184, and 288 cm, using a standard accelerator mass spectrometer (AMS) method (Table 2). The conventional ages for these dated levels are 510 ± 40 , 670 ± 40 , and 1320 ± 40 YBP respectively, and are calibrated to calendar years according to INTCAL98 (Stuiver et al. 1998), resulting in AD 1410, 1295, and 680.

Table 3 and Fig. 17 show the relationship between the dated ages and calibrated depths from the bottom surface, excluding the thickness of the event sediments. Because the event sediments, such as slump and turbidite, deposit in a very short time but occupy a greater stratigraphic portion, the thickness is subtracted from the observed depths. The straight line determined by the least-square fitting method shows some departures from the dated points (Fig. 17, line A). This discordance may be caused partly by the mixing of old carbon with the organic sediments at depths of 78 and 288 cm. Despite this disparity, this line offers a rough guide to the age estimation of the sediments.

As will be discussed later, the slump deposits at the depths of 76, 178, 288, and 299 cm are considered to be induced by strong earthquake shocks reported in the western Nagano area in AD 1714, 841, and 761 (Usami 1987). These earthquakes roughly correlate with the slump deposits in age, except for that at 178 cm depth. The age of the sudden density peak at 15 cm depth is additional information given by the hydraulic change occurring in the lake system due to hydropower generation near the lake since AD 1954. The relationship between the ages of these events

Table 2. Radiocarbon dating data from Laka Nakatsuna^a

Sample no.	Measured age ($\pm 1\sigma$)	$\delta^{13}\text{C}$ (permil)	Conventional age ($\pm 1\sigma$)	Calibrated age (2σ)	Measured material	Measured no.
Naka3-78	510 ± 40	-25.1	510 ± 40	AD 1420 (1410-1435)	Organic sediment	Beta-137249
Naka3-184	650 ± 40	-23.8	670 ± 40	AD 1295 (1285-1310, 1365-1380)	Plant material	Beta-137250
Naka3-288	1360 ± 40	-27.5	1320 ± 40	AD 680 (665-705)	Organic sediment	Beta-137251

^aAll data were measured by standard AMS method at the Beta Analytical Radiocarbon Dating Laboratory

Table 3. Depth and age of the event sediments in the cored sediment at site 1^a

Event Sediments	Depth (cm)	Calibrated depth (cm)	Event age (AD)	Explanation of historical event
Sandy silt	4-7	4		
Dense layer	10-11	7		
Slump(?)	14	8	1954	start of electric power generation
Dense layer	72-73	64		
Slump	76-77	66	1714	Omachi earthquake
Slump	181-186	165		
Dense layer	188-191	168		
Slump	269-283	249	841	destructive earthquake
Slump(?)	299-315	264	762	destructive earthquake

^aThe relationship between calibrated depth and estimated event age is illustrated in Fig. 17 as line B

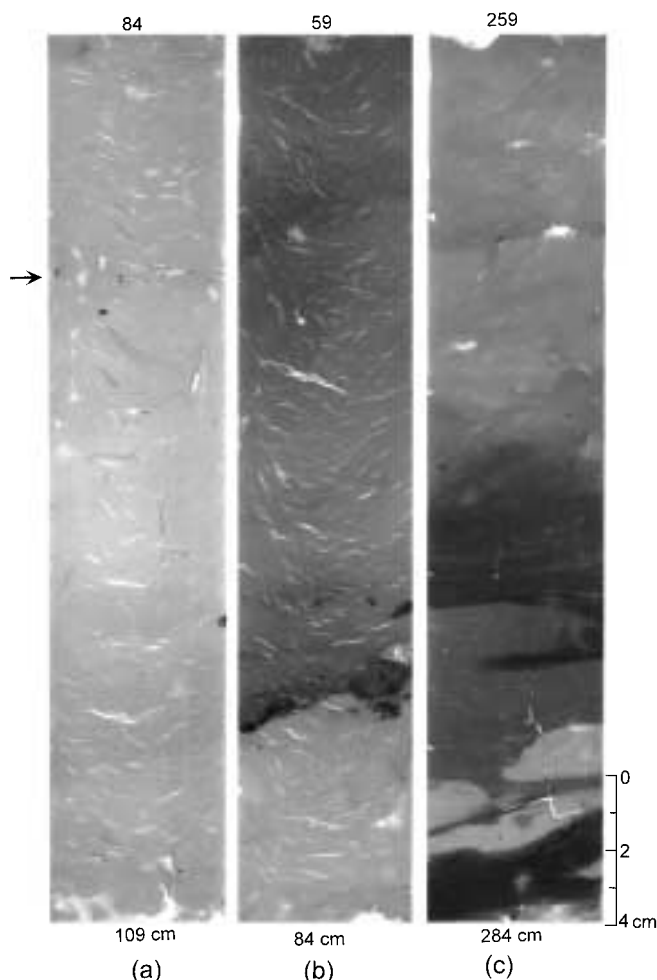


Fig. 13. X-ray photographs of selected parts of the cored sediments. **a** 84 to 109-cm core section with arranged distribution of granules and sands in the sediment as indicated by *arrow*; **b** 59 to 84-cm core section showing denser interval with sharp basal boundary and basal mud clasts; **c** 259 to 248-cm core section showing slump with contorted boundaries in the sediment

and calibrated depths provides a good concordance and validates the above-mentioned assumption (Fig. 17, line B). We use this line as an age reference in the following discussion, which yields an average sedimentation rate of 2 mm year^{-1} ($66 \text{ mg cm}^{-2} \text{ year}^{-1}$).

Discussion

Modern hydraulic conditions

The results of grain-size analysis revealed a clear correlation between water depth and distribution of surface sediments, with decreasing grain size towards the basin center (Figs. 4 and 8B). Current and wave activities induced by stream flow and wind stress influence only the peripheral shallow zone (less than 6 m) and the stream mouth area, as indicated by the presence of winnowed lag deposits of gravel to sand (Fig. 8B). With increasing distance from the shore, hydraulic energy decreases towards the center, which

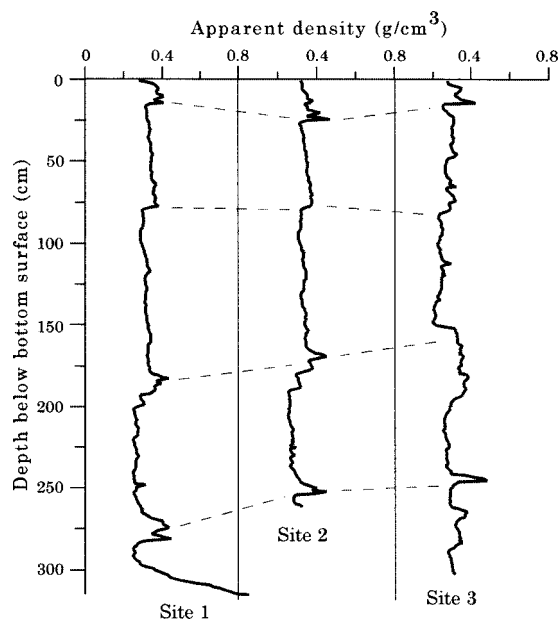


Fig. 14. Density profiles at the three sites in Lake Nakatsuna. Apparent density means solid weight per unit space calculated from dry weight and water content

facilitates the deposition of finer sediments in the basin through suspension. The fine and coarse tails in the size-frequency distribution and the generally poor sorting of the sediments (Fig. 9) suggest mixing of sediments under more than one hydraulic regime as a result of seasonal change in the hydrographs of the inflowing streams, although there was no distinct lamination in the sediments. Winter climate is also an important factor influencing sediment texture and distribution, because snow melt supplies sediments to the frozen lake surface even before the onset of spring. The granule and sand grains scattered in the sediments are dropstones settled through surface ice melting. The contents of TOC and TN in the bottom surface sediments are positively correlated with the clay content, which indicates that the organic materials accumulate with clay through suspension. The sediments of higher C/N ratios are distributed in the inshore zone, suggesting a higher influence of terrestrial plant detritus.

Causes of density change

Judging from the pattern of internal variations, there are three types of density changes: short-term slight increases, long-term decreasing trends with abrupt increases at the base, and large basal increases.

The horizons of short-term slight increases have slightly higher proportions of granule, sand, and/or coarse silt than those of other parts, whereas the variations of TOC, TN, and C/N ratio are insignificant. The coarse grains are scattered in clayey sediments, forming faint layers (Fig. 13a). This occurrence suggests that coarse particles and fine clayey materials are settled independently by different mechanisms. A possible mechanism for the settling of coarse particles is a fall from ice rafts. Abundant snow-melt

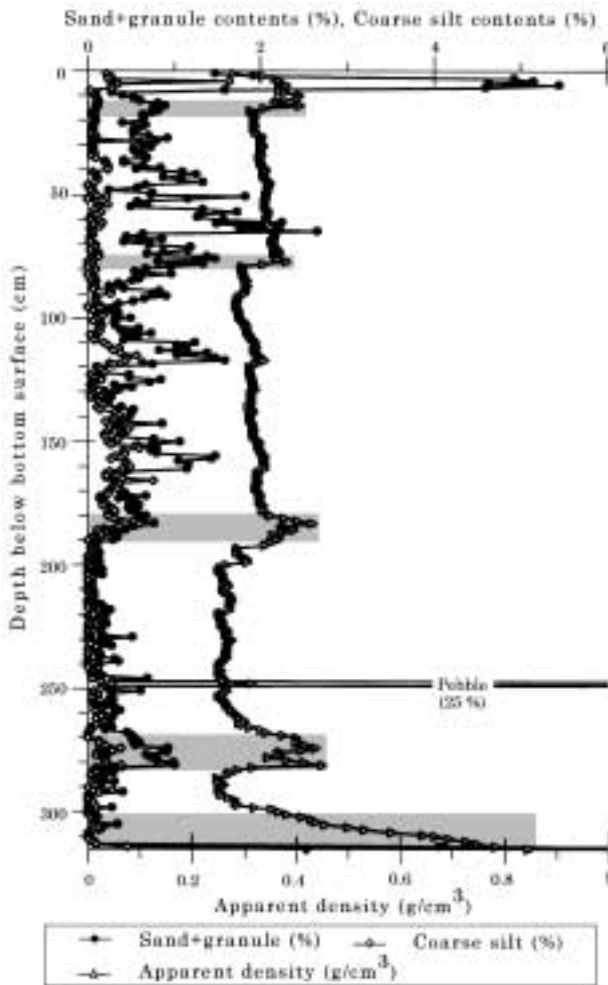


Fig. 15. Sand + granule, coarse silt, and apparent density profiles at site 1 in Lake Nakatsuna. Shaded parts indicate the event sediment intervals

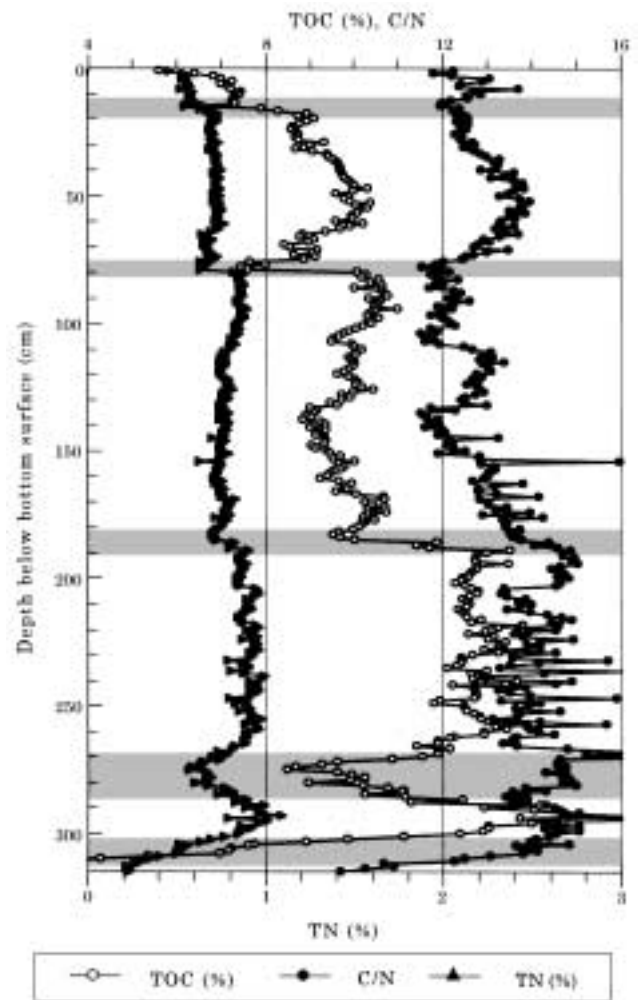


Fig. 16. Distribution of TOC, TN, and C/N weight ratio with depth in the cored sediments at site 1. Abbreviations are as in Figs. 10 and 11. Shaded parts indicate the event sediment intervals

can wash out coarse sediments on the icebound lake surface in early spring. Snow slides may also transport large particles on the icebound lake surface. When the ice sheet is broken into pieces by wind stress in spring, ice blocks near the coast drift to the center of the lake, carrying coarse materials. This process could deposit coarse particles at the center, as do icebergs in the northeast Atlantic Ocean (Heinrich et al. 1988). Except for the short-lived intervals of event sediments, the proportion of coarse fraction is therefore considered as an indicator of winter snow accumulation and lake surface freezing.

The base of the long-term decreasing trend is characterized by sudden increases in density (Fig. 18) that contain small amounts of sand. For these horizons, X-ray photographs show less transparent layers and/or contorted bedding (Fig. 13b and c). The contorted structures suggest slumping during the sedimentary process. The estimated date of the high-density horizons from 269 to 283 cm is about AD 720 on the basis of the depth-age line (Fig. 17, line A). Historical documents record the occurrence of destructive earthquakes in western Nagano in AD 762 and 841

(Usami 1987). The trench survey of the Itoigawa-Shizuoka Tectonic Line also revealed fault activity around the Omachi-Hakuba area about AD 800 (Okumura et al. 1995). Therefore, the contorted dense horizon from 269 to 283 cm is most probably slump deposits induced by the earthquake of AD 762 or 841.

Similarly, the high-density horizon from 76 to 78 cm depth is less transparent with basal mud clasts in X-ray photographs, and the age is estimated as AD 1670 based on line A in Fig. 17. Therefore, it may correspond to the Omachi earthquake of AD 1714 ($M = 6.3$). The lowermost horizon from 299 to 315 cm has an especially high density with very low contents of sand, TOC, TN, and C/N ratios. These features can also be explained as earthquake-induced slump deposits. The date of this event is about AD 650 on the basis of line A. If these three event sediments can be attributed to the historical earthquakes of AD 762, 841, and 1714, respectively, these three events show a good relation between depth and age (Fig. 17, line B). The event of artificial modification in 1954, the start of hydropower generation, is also located on line B. The

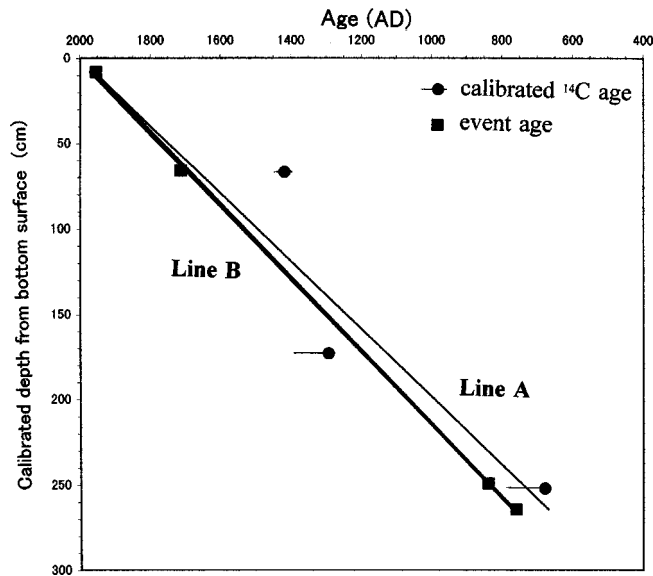


Fig. 17. Depth-age relationship of the cored sediments at site 1. Lines A and B are based on calibrated ^{14}C and event ages, respectively. Event descriptions are given in Table 3

date of the event horizon from 181 to 186 cm is estimated to be about AD 1200, based on line B in Fig. 17, but there are no documented records of the event around that period. This may be due to the lack of historical records caused by the social disturbance at the end of the Heian Period.

The density decreases upward gradually in the long-term decreasing trend. This may be partly due to the higher sand content at the basal horizon. A destructive earthquake corresponding to the basal event sediment caused landslides in the drainage area of the lake. The disturbed land surface produced abundant clastic materials, resulting in a high supply of sediments to the lake. Later, the recovery of vegetation in the land surface of the drainage basin reduced the supply of clastic materials. These factors are another explanation for the relatively high density and its upward decrease.

The uppermost part above 15 cm depth is explained by the recent construction of a channel to utilize the water of Lake Aoki for electric power generation in 1954. The sudden increase in density reflects the effects of the construction and the start of power generation. Recent road construction and opening of ski fields are other factors that increase clastic sediment, resulting in higher density with some sudden peaks.

Meaning of TOC and TN contents

Organic matter in the lake sediments may be derived from lake plankton and terrestrial plants. The nonvascular aquatic plants have C/N ratios of about 6 to 8, whereas vascular land plants, which contain cellulose, have C/N ratios above 30 (Nakai and Koyama 1987). The distribution of C/N ratios in the surface sediments indicates that the contribution of land plants decreases towards offshore, with a minimum of 11 at the lake center (Fig. 11). Therefore, TOC and TN in the cored sediments, which have C/N ratios between 11 and 15, is considered to be a mixture of lake

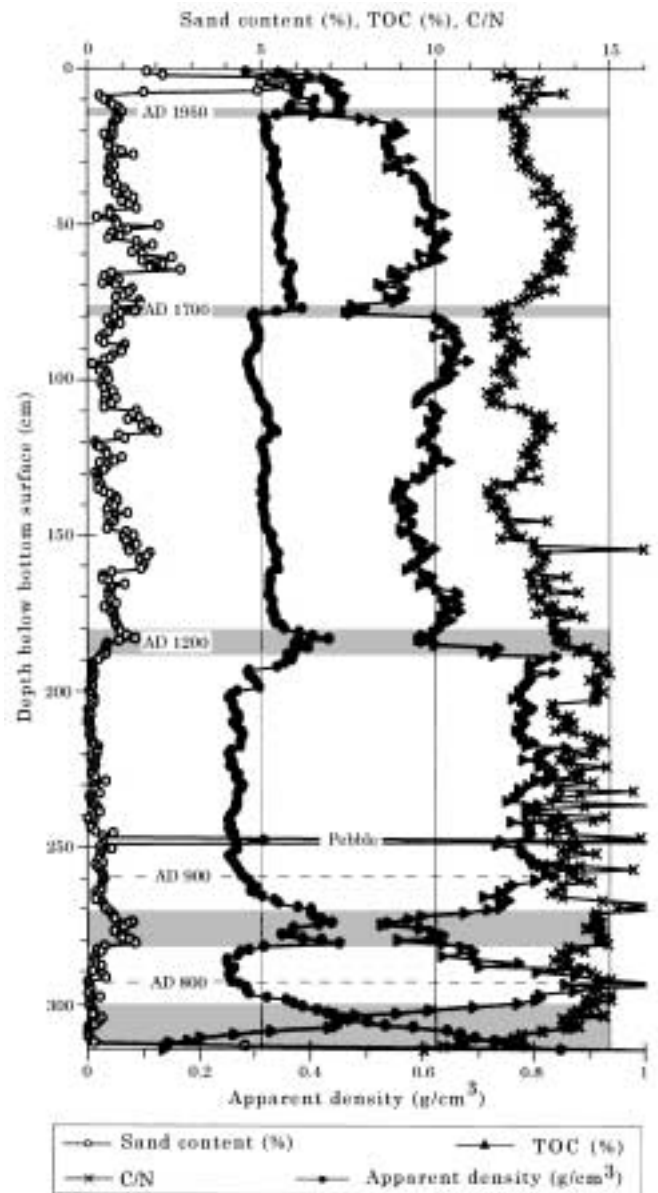


Fig. 18. Relationships among sand content, TOC, C/N, and apparent density. Ages are based on the depth-age relationship shown in Fig. 17, line B. Age boundaries are placed where the TOC contents show remarkable changes. Abbreviations are same as in Figs. 10 and 11. Shaded parts indicate the event sediment intervals

plankton and terrestrial plants, but the former seems to be predominant.

Except for the event sediments, a distinct difference in TOC and TN contents existed between 259 to 180 and 180 to 15 cm depths (Fig. 16). High TOC (12%–13%) and TN (0.9%–1%) with higher C/N ratios characterize the former horizon, whereas low TOC (9%–11%) and TN (0.8%–0.9%) correspond to the latter (Fig. 16). The reduction is more than 20%. Because the sedimentation rate is almost constant (Fig. 17), this reduction is considered to be a true decrease in the rate of accumulation of organic matter.

The further reduction in TOC and TN contents above 15 cm is attributable to the artificial mixing of cold water

into the lake in 1954, which reduced the production of organic matter in the lake water. A recent study on the productivity of phytoplankton in the water of Lake Suwa reported a sharp reduction of chlorophyll *a* in the cool summer of 1993, when solar radiation was decreased, and an increase in the hot summer of 1994, when solar radiation was above average (Park et al. 1998). For lakes situated in regions with forested catchment areas, climate warming has been reported to produce an increase in the concentration of dissolved organic carbon (DOC) in lake waters (Battarbee 2000). Monitoring of upland lakes in the UK over the last decades showed a consistent increase in DOC and sediment TOC content, which has been linked to the recent temperature increase (Battarbee 2000). These modern analogues support the concept that abundant TOC and TN are produced in warm climates, probably during hot summers.

Long-term fluctuation in TOC and TN contents corresponds to the general cool-warm cycles of the glacial-interglacial changes, with higher TOC contents for the warm Holocene sediments (Inouchi et al. 1996; Kumon et al. 2000). Pollen analysis also clarified the correspondence between high TOC and TN and warm climate in the sediments of Lake Nojiri, based on the same specimen used for carbon, and nitrogen (CHN) analysis (Kumon et al. 2000). As discussed above, it is reasonable to conclude that the high and low concentrations of TOC and TN in the sediment record of Lake Nakatsuna also indicate relatively warm and cool periods.

Climatic changes during the last 1300 years

The two intervals from 259 to 180 cm and from 180 to 15 cm are characterized by distinct differences in TOC, TN, and sand contents and correspond to AD 900 to 1200 and 1200 to 1950, respectively (Fig. 17, line B). Therefore, the sedimentary history of Lake Nakatsuna is divided into two major climate phases.

AD 900–1200

High TOC, TN, and diatom concentrations, combined with low sand content, characterize the three centuries between AD 900 and 1200 (Figs. 16 and 18). These high concentrations indicate the existence of warm climatic conditions, most probably hot summers. Low sand content, on the other hand, implies little ice bounding and less snow accumulation around the lake, and suggests warm winters. In the meteorological record of the last 28 years at Omachi station, summer temperature is inversely correlated with summer precipitation (Fig. 3). Based on this relationship, if the summers were hot during AD 900–1200, summer precipitation might have been low. According to this view, the climate during AD 900–1200 in central Japan was warm, with warm winters, hot summers, and low summer precipitation.

The climate of western Europe for the period encompassing AD 800–1300 is called the Medieval Warm Period (MWP) (Hughes and Diaz 1994). Although the MWP was experienced in different parts of the world, its timing and

duration vary among researchers and regions. Research on the ice core from central Greenland supports the existence of a stable MWP between AD 600 and 1000, 200 years earlier than in Europe (Meese et al. 1994). In a tree-ring-based study, Stine (1994) reported that the MWP in California had two phases, AD 892–1112 and 1209–1350. Records of sediment grain size from Pine Lake, Canada, yield timing of the MWP as AD 700–1300 (Campbell 1998).

Based on pollen analysis, Sakaguchi (1983) first clarified the existence of warm climatic conditions in Japan in the period AD 700–1300. On the basis of $\delta^{13}\text{C}$ record of tree rings at Yakushima Island, southern Japan, Kitagawa and Matsumoto (1995) have placed the MWP at AD 750–1300. Inouchi et al. (1996), Fukusawa (1996), and Kumon (2001) have also reported the existence of the MWP based on analysis of lake sediments. Our data suggest warm climatic conditions between AD 900 and 1200, which corresponds to the MWP.

AD 1200–1950

Between AD 1200 and 1950, after the MWP, the abrupt decrease in TOC and TN and the increase in sand content (Figs. 16 and 18) suggest that the climate shifted to another mode. Low summer temperatures with less solar radiation might have reduced TOC and TN contents. The effect of cold winters might increase snow precipitation and icebounding, which yield a high proportion of sand grains as dropstones through ice drifting. Therefore, cool climatic conditions imply the combination of mild or cool summers and cold winters, but the degree of coolness varied, as evidenced by the fluctuating TOC and TN profiles. The period spanning AD 1200–1950 includes three notably cool periods from AD 1300 to 1470, 1700 to 1760, and 1850 to 1950, and three moderately cool periods between the these cool phases.

Evidence presented by Fukusawa (1996) suggests a cool phase between AD 1580 and 1880, which is the Little Ice Age (LIA) as defined by Mikami (1992). In connection with the LIA, the seventeenth and the nineteenth centuries in the northern hemisphere were cool (Bradley and Jones 1992). In the GISP2 record, the LIA is not as well defined as the MWP; periods of lower and higher temperatures have occurred over the last 800 years, and the perception of the LIA as a period of sustained cold is not supported (Meese et al. 1984). Carbon isotope study of Japanese cedar clarified the timing of the LIA between AD 1600 and 1800 (Kitagawa and Matsumoto 1995). In our view, the early cooling starting around AD 1200 can be viewed as the initial onset of the LIA, but it was not a sustained cold period. In the latter two cool phases, AD 1700–1760 and 1850–1950 reported here, the recessions in TOC, TN, and diatom concentration are notable and are considered to be symptomatic of the cold climatic condition related to the LIA.

Historically, the LIA in Japan is widely correlated with the Edo Period (1603–1868), during which three major famines, Kyoho (1732), Tenmei (1782–1787), and Tenpou (1832–1837) occurred because of the climatic anomaly (Fukuoka 1992; Sugihara and Yamakawa 1992). It was

characterized by rainy and cool summers that badly reduced the rice crop. Another pattern was a tendency for mild winters combined with cool summers and cold winters with mild summers (Fukaishi and Tagami 1992). Although the climate mechanism of the cool phase and the link to the LIA remain controversial (Bradley and Jones 1992), both the findings of this study and the historical records mentioned above are consistent with the existence of cool climatic conditions in the thirteenth to the fifteenth centuries and in the seventeenth and nineteenth centuries.

Conclusions

A mesotrophic Lake Nakatsuna is dimictic, and its hypolimnion is anoxic during thermal stratification. The distribution of surface sediments reveals a clear correlation with the bathymetry and hence with the water depth with decreasing grain size toward the basin center. The content of sand and granule grains scattered in the sediments is largely controlled by the extent of icebounding and snow accumulation in and around the lake during the winter. Cored sediments from this lake record a climate-modulated history of the past 1300 years in central Japan, and the overall picture that emerges from comparison among proxy records has been translated into the two qualitative paleoclimate phases. A relatively warm climate phase occurred during AD 900–1200. This period was warmer than any other period during the last 1300 years, which corresponds to the MWP climate anomaly. Climate cooling began around AD 1200, and greater fluctuations appeared as time progressed. During the period from AD 1200 to 1950, three cool phases are recognized: AD 1300–1470, 1700–1760, and 1850–1950. The middle and late parts of this cool phase correspond with the LIA.

Acknowledgments We thank S. Tanabe, B.K. Adhikari, M. Takabatake, K. Kanamaru, M. Khobayashi, A. Yoda, M. Kasuga, A. Chigira, T. Sakai, T. Okusawa and T. Yoshikawa for their assistance in the field sampling and laboratory analysis, and T. Arai and A. Yokoyama for their helps in various ways. Thanks are also due to Prof. Y. Inouchi, Prof. H. Hayashi and Dr. N. Murakoshi who offered many helpful comments. Thanks are particularly expressed to U.K. Aryal and H.C. Oscar for language revision. The constructive comments of two anonymous reviewers are much appreciated.

References

- Battarbee RW (2000) Paleolimnological approaches to climate change, with special regard to the biological record. *Quat Sci Rev* 19:107–124
- Bradley RS, Jones PD (1992) When was the “Little Ice Age”? In: Mikami T (ed) *Proceed Internat Symp on Little Ice Age Climate*, pp 1–4
- Campbell C (1998) Late Holocene lake sedimentology and climate change in south Alberta, Canada. *Quat Res* 49:96–101
- Fukaishi K, Tagami Y (1992) An attempt of reconstructing the winter weather situations from 1720 to 1869 by the use of historical documents. In: Mikami T (ed) *Proceed Internat Symp on Little Ice Age Climate*, pp 194–201
- Fukuoka Y (1992) The dendroclimatological study on the Little Ice Age in Japan. In: Mikami T (ed) *Proceed Internat Symp on Little Ice Age Climate*, pp 71–74
- Fukusawa H (1996) High-resolution reconstruction of environmental changes from the last 2000 years varved sediments in Lake Suigetsu, central Japan. In: Mikami T, Matsumoto E, Ohta S, Sweda T (eds) *Proceed 1995 Nagoya IGBP-PAGES/PEP-II Symp*, pp 84–89
- Heinrich H (1988) Origin and consequences of cyclic ice rafting in the northeast Atlantic Ocean during the past 130000 years. *Quat Res* 29:142–152
- Horie S (1962) Morphometric features and the classification of all the lakes in Japan. *Mem Col Sci, Kyoto Univ, Ser B* 24:191–262
- Hughes MK, Diaz HF (1994) Was there a “Medieval Warm Period”, and if so where and when? *Climate Change* 26:109–142
- Inouchi Y, Yokota S, Terashima S (1996) Climatic changes around Lake Biwa during the past 300000 years and 2000 years. In: Mikami T, Matsumoto E, Ohta S, Sweda T (eds) *Proceed 1995 Nagoya IGBP-PAGES/PEP-II Symp*, pp 109–114
- Kitagawa H, Matsumoto E (1995) Climatic implications of $\delta^{13}\text{C}$ variations in a Japanese cedar (*Cryptomeria japonica*) during the last two millennia. *Geophys Res Lett* 22:2155–2158
- Kumon F (2001) Paleolimnological studies. In: Saijo Y, Hayashi H (eds) *Lake Kizaki, Backhuys, Leiden*, pp 55–62
- Kumon F, Kamitani T, Sutoh K, Inouchi Y (1993) Grain size distribution of the surface sediments in Lake Biwa, Japan (in Japanese). *Mem Geol Soc Jpn* 39:53–60
- Kumon F, Ohno R, Sakai T, Sakami S, Sakai J (2000) Climatic records during the last 40000 years in Lake Nojiri, central Japan. In: Mikami T (ed) *Proceed Internat Conf on Climate Change and Variability*, pp 41–44
- Meese DA, Gow AJ, Grootes P, Mayewski PA, Ram M, Stuiver M, Taylor KC, Waddington ED, Zielinski G (1994) The accumulation record from the GISP2 core as an indicator of climate change throughout the Holocene. *Science* 266:1680–1682
- Mikami T (1992) Climatic variation in Japan during the Little Ice Age. In: Mikami T (ed) *Proceed Internat Symp on Little Ice Age Climate*, pp 176–181
- Nagano Research Institute for Health and Pollution (1983) Present condition of Nishina Three Lakes. In: *Preservation of the natural condition of Nishina Three Lakes and the surrounding river systems* (in Japanese). Omachi City Office, pp 44–45
- Nakai N, Koyama M (1987) Reconstruction of paleoenvironment from the viewpoints of the inorganic constituents, C/N ratio and carbon isotopic ratio in the 1400 m core taken from Lake Biwa. In: Horie S (ed) *History of Lake Biwa. Kyoto Univ Contrib* 553:137–156
- Okumura K, Imura R, Imaizumi T, Sawa H, Togo M (1995) Paleoseismological study of the Itoigawa-Shizuoka tectonic line active fault system (in Japanese). *Geol Sur Jpn, Res Data No* 259:89–98
- Park HD, Iwami Chi, Watanabe MF, Harada K, Okino T (1998) Temporal variabilities of the concentration of intra- and extracellular microcystin and toxic microcystis species in a hypertrophic lake, Lake Suwa, Japan (1991–1994). *Environ Toxicol Water Qual* 13:61–72
- Sakaguchi Y (1983) Warm and cold stages in the past 7600 years in Japan and their global correlation – especially on climatic impacts to the global sea level changes and the ancient Japanese history. *Bull Depart Geogr, Univ Tokyo* 15:1–31
- Shepard FP (1954) Nomenclature based on sand-silt-clay ratios. *J Sed Petr* 24:151–158
- Stine S (1994) Extreme and persistent draught in California and Patagonia during Medieval time. *Nature* 369:546–549
- Stuiver M, Reimer PJ, Bard E, Beck W, Burr GS, Hughen KA, Kromer B, McCormac G, Plicht JVD, Spurk M (1998) Intcal98 radiocarbon age calibration, 24000–0 cal BP. *Radiocarbon* 40:1041–1083
- Sugawara K, Seiji S, Chushiro K (1937) Analysis of dissolved gasses in lake water and notes on lake metabolism (Part 1) (in Japanese). *J Chem Soc Jpn* 38:890–903
- Sugihara Y, Yamakawa S (1992) The relationship between environmental changes and Japanese rice yield since the latter half of Little Ice Age. In: Mikami T (ed) *Proceed Internat Symp on Little Ice Age Climate*, pp 202–207
- Usami T (1987) Materials for comprehensive list of destructive earthquakes in Japan (in Japanese). University of Tokyo Press, Tokyo
- Yoshimura S (1938) Dissolved oxygen of the lake waters of Japan. *Sci Rep Tokyo Bunraku Daigaku, Sec C*, 2:63–77